2015 年 8 月
碩士學位論文

Synthesis and physicochemical characteristics of hydroxyapatite-derived from abalone shell

朝鮮大學校 大學院

齒醫生命工學科

康 倧 綠

전복 패각에서 유래한 수산화인회석의 합성과 물리 화학적 특성

Synthesis and physicochemical characteristics of hydroxyapatite-derived from abalone shell

2015年 8月 日

朝鮮大學校 大學院

齒醫生命工學科

康 倧 綠

Synthesis and physicochemical characteristics of hydroxyapatite-derived from abalone shell

指導敎授 金 秀 官

이 論文을 理學碩士學位신청 論文으로 提出함.

2015年 4 月

朝鮮大學校 大學院

齒醫生命工學科

康 倧 綠

康倧綠의 碩士學位論文을 認准함

委員長　朝鮮大學校　敎　授　김도경 印

委　員　朝鮮大學校　敎　授　김수관 印

委　員　朝鮮大學校　敎　授　김춘성 印

2015年 5 月

朝鮮大學校 大學院

Contents

List of Figures

List of Abbreviations

Distilled water	DI
Canning electron microscopy	SEM
Energy dispersive spectrometry	EDS
X-ray diffraction	XRD
Fourier-transform infrared	FT-IR
Human MG-63 osteosarcoma cells	MG-63 cells
Korea cell line bank	KCLB
Dulbecco's modified Eagle's medium	DMEM
Fetal bovine serum	FBS
-(4, 5-dimethylthiazol-2-yl)-2, 5-diphenyltetrazolium bromide	MTT
Dimethylsulfoxide	DMSO
4'6-diuamino-2-phenylindole dihydrochloride	DAPI
Dulbecco's phosphate-buffered saline	DPBS
Alkaline phosphatase	ALP
β-tricalcium phosphate	β-TCP

국문초록

전복 패각 유래한 수산화 인회석의 합성과 물리 화학적 특성

강경록

지도교수 : 김수관

조선대학교 치의생명공학과 석사과정

본 연구에서는 전복 패각으로부터 수산화인회석을 합성하여 이에 대한 물리 화학적 특성과 생물학적 안정성 평가를 통하여 향후 치과 의료용 합성골 이식재 재료를 개발하는 효용성 분석을 목적으로 한다. 이에 따라 전복 패각으로부터 합성된 수산화인회석의 분석을 위하여 한국 식품 의약품 안전처 (Ministry of Food and Drug Safety, MFDS)와 한국 식품의약품 안전평가원 (National Institute of food and Drug Safety Evaluation, NiFDS)에서 제공한 의료기기 평가가이드라인에 의거하여 생물학적, 물리·화학적 특성을 분석하였다.

본 연구를 위하여 완도에서 수집한 전복 패각의 오염물을 제거하기 위하여 1차 증류수 속에 넣고, 초음파세척기(JAC-4020, KODO, Seoul, Republic of Korea)에서 60 분간 초음파 세척을 실시하였다. 1차 세척된 전복 패각을 과산화수소 용액 하에서 90 분간 초음파 세척 실시 후, 잔여 과산화수소를 세척하기 위하여 60 분간 1 차 증류수로 초음파 세척을 실시 한 후 48시간 동안 완전 건조하여 사용하였다. 산화칼슘 합성을 위하여 전복 패각을 전기로(MF-22G, JEIO TECH, Seoul, Republic of Korea)에 넣고 1시간 당 100℃ 승온하여, 950℃에서 3 시간 소결을 실시하였다. 소결 되어 합성된 산화칼슘은 53㎛ 이하의 분말만을 체 거름하여 실험에 사용하였다. 생성된 전복 패각 유래 산화칼슘을 1 차 증류수에 넣고 0.3 M의 인산을 이용하여 인산화를 진행하였다. 인산화 과정 후 생성된 슬

러리는 화학 잔기를 제거하기 위하여 수차례 3차 증류수를 이용하여 여과한 뒤 50℃에서 24 시간 완전 건조하였다. 건조된 슬러리는 전기로에서 시간당 100℃ 승온하여 1230℃에서 3 시간 소결하여 수산화인회석을 합성하였다.

전복 패각 유래 수산화인회석은 주사전자현미경(SEM, JSM 840-A, JEOL co., Japan) 으로 합성 후 표면 분석을 실시하였으며, 에너지 분광분석기 (Energy-Dispersive Spectroscopy, EDS, XS-169, Japan)을 사용하여 Ca/P 비율을 측정하였다. 또한 X-선 회절 분석기 (X-Ray Diffraction, XRD. X'pert PRO MRD, PAN alytical co. The Netherlands)를 통하여, 구조 결정성을 분석 하였으며, 적외선 분광 분석기(Fourier transform infrared spectroscopy, FT-IR; Nicolet 6700, Thermo Electron, USA) 분석을 통하여 화학적 특성을 평가하였다.

세포 배양은 Dulbecco's modified Eagle's medium (DMEM, Life Technologies, GRAND Island, NY, USA)배지에 growth factor를 제공하는 10% (w/v) Fetal Bovine Serum (FBS, Life Technologies, Grand Island, USA)을 혼합하여 5% CO_2가 공급되는 37℃ CO_2 incubator에서 48 시간 배양하여 사용하였다. 세포독성 평가를 위하여 MTT assay cell live & Dead assay를 수행 하였으며, 조골세포 분화능 평가를 위하여 Alkaline phosphatase (ALP) assay와 Alizarine Red S (Sigma - Aldrich Corp., St. Louis, MO, USA) staining을 수행하였다.

전복 패각 유래 수산화인회석은 주사전자현미경 관찰시, 판상형의 형태를 나타내는 것을 확인 할 수 있었다. EDS 분석을 통한 원소 분석 결과, 소량의 Na 이온이 첨가 되어 있는 것을 제외한 모든 성분이 시판되고 있는 수산화인회석과 거의 동일하였으며 시료 내의 Ca/P 비율 동안 거의 동일함을 확인 할 수 있었다. X-선 회절 분석기를 통한 X선 결정성 분석 평가 결과 시판되고 있는 수산화인회석과의 결정성이 동일함을 확인 하였다. 또한 화학 작용기 확인을 위해 실시한 적외선 분광 분석기 분석 결과 대조군과 동일한 화학 작용기를 확인 할 수 있었다. 체내 독성 평가를 위하여 실시한 MTT 및 Cell live & Dead assay 분석 결과 전복 패각 유래 수산화인회석은 시판되고 있는 수산화인회석에 비해 높은 세포 생존률을 가지며, 대조군과 비교 하였을 때에도 높은 세포 생존률을 확인 할 수 있었다. 전복 패각 유래 수산화 인회석에 의한 골형성능을 분석하기 위하여 인간유래 조골세포인 MG-63 세포에 14 일간 처리 후 ALP assay를 수행한 결과 시판되고 있는 수산화인회석 및 대조군 수준의 골형성능을 확인하였으며, Alizarine Red S Staining을 통하여 고모세포의 무기질화 (Mineralization)를 확인 하였을 때 시판되고 있는 수산화 인회석 수준과 동일함을 확인할 수 있었다.

전복 패각 유래 수산화인회석은 비교 대상인 시판되고 있는 수산화인회석과 물리적, 화학적 특성이 매우 유사하며, 세포 독성 평가에서도 높은 세포 생존률을 확인 할 수 있음에

따라, 향후 치과 의료용 합성골 이식재 개발에서도 우수한 생체 적합성을 가진 생체 재료로서 사용 가능할 것으로 사료된다.

Ⅰ. Introduction

Bone comprises the structure of the body and consists of inorganic compounds. Even though bone is quite rigid and has self-healing mechanisms, it it is susceptible to damage by trauma, cancer, or disease [1]. The biological mechanisms that provide a rationale for bone grafting are oseteoconduction, osteoinduction, and osteogenesis. Osteoconduction occurs when the bone graft material serves as a scaffold for new bone growth that is perpetuated by the native bone. Osteoinduction involoves the stimulation of osteoprogenitor cells to differentiate into osteoblasts, which then begin new bone formation. Osteogenesis occurs when viable osteoblasts originating from the bone graft material contribute to new bone growth along with the bone growth generated via the other two mechanisms [2].

Guided bone regeneration (GBR) is a well-established method to exclude soft-tissue cells by means of a barrier membrane [3]. When a large quantity of bone is required, GBR is performed before implant placement. Bone grafting materials are currently in use to treat patients. Among the many bone grafting materials available, synthetic ones are the most versatile for dental surgery [4].

Autogenous bone grafting involves the use of bone obtained from the same individual receiving the graft. Autogenous bone is most generally preferred because there is less risk of graft rejection as the graft originated from the patient's body. On the other hand, this surgery carries added risks. For example, a separate incision is made and a small piece of bone is removed from an area of the body where it is not needed, which can be associated with increased morbidity and wound-site infections [5].

Allograft bone, like autogenous bone, is derived from humans, the difference being that allografts are harvested from an individual other than the recipient. However, allografts have some potential problems such as disease transmission (either viral or bacterial), tumor transplantation, and immune rejection [6].

A xenograft bone substitute originates from a species other than human, such as bovine or porcine, which can be freeze dried or demineralized and deproteinized. Xenografts are normally distributed only as a calcified matrix [7].

Synthesized bone materials can be produced from ceramics, such as calcium phosphate, hydroxyapatite (HA), tricalcium phosphate, bioglass, and calcium sulphate, all of which are biologically active to different degrees depending on their solubility in the physiological environment [8]. These materials can be doped with growth factors, ions such as strontium, or mixed with bone marrow aspirate to increase their biological activity. However, some studies have suggested that this method is inferior to autogenous bone grafting.

Abalone shells are used as decorative items and as a source of jewelry, buttons, buckles and inlays, but the vast majority are discarded and are environmental pollutants. Every year, the tipping fees for the proper disposal of waste abalone shell are particularly high. Therefore, the recycling of waste materials using low-cost technology to produce biocompatible materials, such as HA from abalone shell, is an important development.

The aim of this study was to verify the physicochemical characteristics and cellular biocompatibility of abalone shell-derived HA for use as a bone grafting material. This study provides a method for obtaining HA from abalone shell, its characterization, and a demonstration of its biocompatibility.

Ⅱ. Materials and Methods

Ⅱ-A. Synthesis of Hydroxyapatite

The processing steps to synthesize HA from the shells of *Haliotis* sp. abalone are briefly illustrated in Fig. 1.

Ⅱ-A-1. Preparation of abalone shells

Haliotis sp. shells used in this study were randomly collected from a commercial seafood market in Wando, Republic of Korea. The contaminants attached to the abalone shell were removed with water using an ,ultrasonicator (JAC-4020, KODO, Seoul, Republic of Korea) for 60 min at room temperature, which was repeated three times. The shells were then washed with hydrogen peroxide in the ultrasonicator for 90 min at room temperature, followed by washing with water in the ultrasonicator for 60 min at room temperature to remove the hydrogen peroxide. Next, the abalone shells were dried for 48 h at room temperature and were then crushed into powder in a Wonder Blender (WB-1, Kastech, Japan).

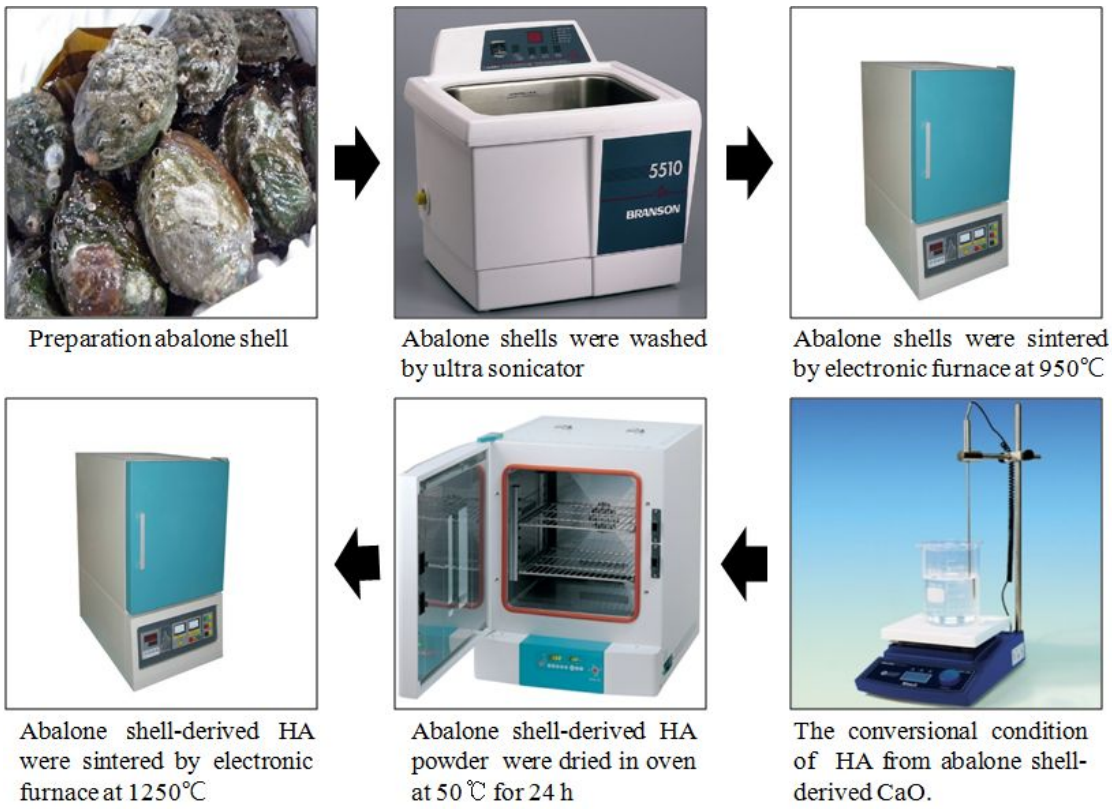

Figure 1. Schematic diagram of HA synthesized from abalone shell.

Ⅱ-A-2. The sintering condition for preparing the calcium oxide from abalone shells

To obtain calcium oxide (CaO), the powdered abalone shell was sintered in an electronic furnace (MF-22G, JEIO TECH, Seoul, Republic of Korea) at 950°C for 3 h. After sintering, CaO ≤ 53 μm in size was collected using a mesh sieve. Finally, residues were investigated by comparison with commercial CaO (Sigma - Aldrich, St. Louis, MO, USA).

Ⅱ-A-3. The conversional condition of Hydroxyapaptite from CaO

To synthesize $Ca(OH)_2$,CaOsinteredfromabaloneshellswas dissolved in deionized (DI) water by stirring with a magnetic bar at 300 rpm. After dissolution, 0.3 M phosphoric acid was added dropwise into the CaO solution while maintaining a pH of 10.5. The reacted residues were washed with DI water to remove the impurities, filtered through filter paper, and dried in an drying oven at 50°C for 24 h. Finally, the residues were sintered in an electronic furnace at 1230°C for 3 h. After sintering, the residues were investigated by comparison with commercial HA (Sigma - Aldrich Corp., St. Louis, MO, USA)

Ⅱ-B. Evaluation of physical and chemical properties

Ⅱ-B-1. Scanning electron microscopy analysis

To observe the morphology of the synthesized HA, samples were sputter-coated (Emitech K550 sputter coater, Emitech Ltd, UK) and were observed by scanning electron microscopy (SEM, JSM 840-A, JEOL, Tokyo, Japan) at 1,000×, 3,000×, and 10,000× magnifications. The Ca/P ratio was examined by energy-dispersive spectrometry (EDS, XS-169, Japan).

Ⅱ-B-2. X-ray diffraction and Fourier Transform Infrared spectroscopy analysis

The crystal structure of the materials was determined by X-ray diffraction (XRD, X'pert PRO MRD, PANalytical, Almelo, The Netherlands) using CuK_aradiation produced at 40 kV and 30 mA. The patterns were scanned from 10 - 60° 2Θ at a scan rate of 2° per minute with a step size of 0.05°. The chemical characteristics were measured by Fourier-transform infrared (FT-IR; Nicolet 6700, Thermo Scientific, Waltham, MA, USA) sperctroscopy.

Ⅱ-C. *In vitro* cytocompatibility

Ⅱ-C-1. MG-63 cell culture

Human MG-63 osteosarcoma cells were obtained from the Korean Cell Line Bank (Seoul, Republic of Korea). MG-63 cells were cultured in Dulbecco's modified Eagle's medium (DMEM, Life Technologies, Grand Island, NY, USA) supplemented with 10% fetal bovine serum (FBS, Life Technologies, Grand Island, NY, USA) in humidified atmosphere containing 5% CO_2 at 37°C.

Ⅱ-C-2. Cell viability

The cell viability was assessed using 3-(4, 5-dimethylthiazol-2-yl)-2, 5-diphenyltetrazolium bromide (MTT, Life Technologies, Grand Island, NY, USA). The MG-63 cells were seeded at a density of 1×10^5cellsperwellin96-well plates and allowed to attach to the wells overnight. After incubation, cultured cells were treated with effluent of the hydroxyapatite in DMEM with 10% FBS for 24, 48, and 72 h at 37°C. After incubation under the defined conditions, 20 μL of 5 mg/mL MTT were added and were incubated for 4 h. The supernatant was subsequently removed, and MTT crystals were dissolved in 200 μL/well dimethylsulfoxide. This solution was transferred into a 96-well plate and the optical density was measured at 540 nm using a spectrometer (Epoch Micro-volume Spectrophotometer System, BioTek, Winooski, VT, USA). Experiments were performed at least three times.

Ⅱ-C-3. Cell attachment

Cell attachment was measured, as previously described, with a LIVE/DEAD Cell Viability Assay, using green calcein-AM and ethidium homodimer-1 (Life Technologies, Grand Island, NY, USA) to stain live and dead cells, respectively. MG-63 cells were treated with HA effluent on chamber slides, stimulated for 24 h, and then stained with green calcein-AM and ethidium homodimer-1 according to the manufacturer's protocol. Cell images were obtained with a fluorescence microscope (Eclipse TE200, Nikon Instruments, Melville, NY, USA). For staining with modified 4′6-diamino-2-phenylindole dihydrochloride (DAPI), the cells were washed twice with 1× Dulbecco's phosphate-buffered saline (DPBS) after removing the medium, and fixed with 4% paraformaldehyde for 15 min. The cell attachment morphology was observed by fluorescence microscopy with the Eclipse TE200 after washing twice with DPBS.

Ⅱ-C-4. Alkaline Phosphatase Assay

MG-63 cells were seeded at an initial density of 5×10^4cells per well in 0.5mL of DMEM. After 168h of culture, the alkaline phosphatase (ALP) activity was measured similarly to the method described in our previous studies. Briefly, after cultivation, cells were collected and lysed in 200 μL PBS containing 0.2% Triton X-100, which facilitates destruction of the plasma membrane, and then homogenized by sonication. The total protein content in cell lysates was determined using a the Micro/Macro BCA assay (Pierce Chemical, Rockford, IL, USA). The ALP activity was assayed using the conversion of the colorless *p*-nitrophenyl phosphate to the colored *p*-nitrophenol according to the manufacturer's protocol (Sigma - Aldrich Corp., St. Louis, MO, USA). The color changes were measured spectrophotometrically at 405 nm. The amount of *p*-nitrophenol produced was quantified by comparison with a standard curve and normalized to the total protein

content in the cell lysate. ALP activity experiments were repeated three times.

Ⅱ-C-5. Alizarine Red staining

For mineralization assays, MG-63 cells at 4, 7, and 10 days of culture were fixed with 70% ethanol for 20 min and stained with 1% alizarin red S (Sigma-Aldrich Corp., St. Louis, MO, USA) in 0.1% NH_4OH at pH4.2-4.4. To quantify the intensity of mineralization, we measured the density of stained nodules by colorimetric spectrophotometry. The stained cells were collected by centrifugation at 13,000 rpm for 10 min at 4°C. Cell lysates were solubilized with 0.5 mL of 5% SDS in 0.5 N HCl for 30 min at room temperature. Solubilized stain (0.1 mL) was transferred to wells of a 96-well plate, and absorbance was measured at 405 nm.

Ⅱ-C-6. Statistical analysis

Statistical analysis was performed by Student's *t*-test using StatView 5.0 software (SAS Institute, Cary, NC, USA), with *p*-values less than 0.05 considered to be statistically significant.

Ⅲ. Results

Ⅲ-A. SEM analysis and EDS mapping analysis of the HA synthesized from abalone shell

Abalone shell was converted to HA, and SEM of the surface morphology showed the formation of structures at an acceleration voltage of 5.5 kV. As shown in Fig. 2, abalone shell-derived HA has a flat-sheet morphology with a particle size in the range of 25 - 50 μm. EDS was used for elemental analysis of the powder at a sintering temperature of 1230°C. Elemental analysis revealed O, P, and Ca for calcium phosphates, as shown in Fig. 3; however, abalone shell-derived HA has little Na. EDS analysis showed that the commercial HA and abalone shell-derived HA have similar elemental compositions.

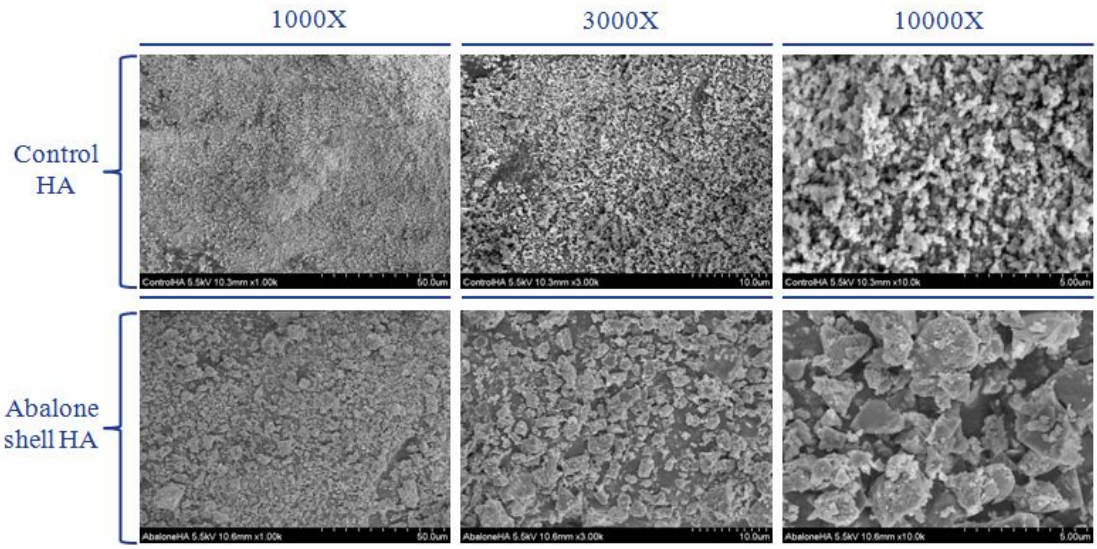

Figure 2. SEM images showing surface appearance of HA sheet. the surface appearance of a HA sheet after sintering was observed by SEM at an acceleration voltage of 5.5 kV(A) 1000 x, (B) 3000 x, (C) 10000 X.

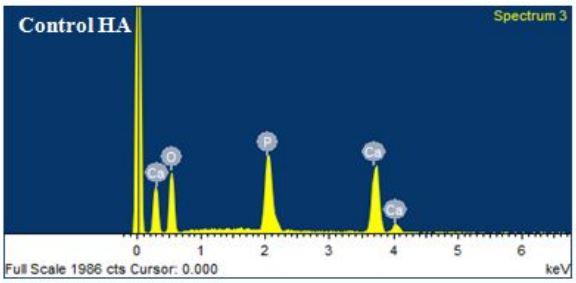

Element	Weight %	Atomic %
O	64.85	80.49
P	14.36	9.21
Ca	20.79	10.30
Total	100	100

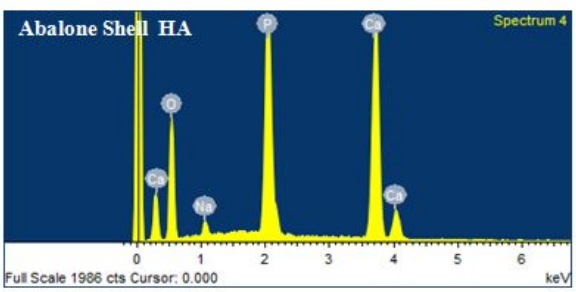

Element	Weight %	Atomic %
O	56.70	74.07
P	16.53	11.15
Ca	24.65	12.85
Na	2.12	1.93
Total	100	100

Figure 3. . EDS analysis of HA synthesized from abalone shell, which shows that the calcium to phosphorous ratio (Ca/P ratio) is 1.83.

Ⅲ-B. Characterization of synthesized HA by sintering at 1230℃ temperatures

The molar amount of CaO needed to produce a certain amount of HA was first calculated using the reaction formula, and then sintering at 1230°C was used to synthesize HA, which was measured by FT-IR analysis. FT-IR spectra were obtained in the range of 500 - 4000 cm^{-1}.The FT-IR spectra for the powders is shown in Fig. 4. The peaks at 1030 and 570 cm^{-1}, which are attributed to PO_4^{3-}, indicate the presence of HA phases. The C-O vibration in the CO_3^{2-} vibration band disappeared and the spectrum obtained was characteristic of HA. Furthermore, Fig. 5 shows the XRD patterns of HA synthesized by sintering at 1230°C, which revealed one unknown peak after sintering. The other peaks were nearly identical. These results show that HA was successfully synthesized at 1230°C.

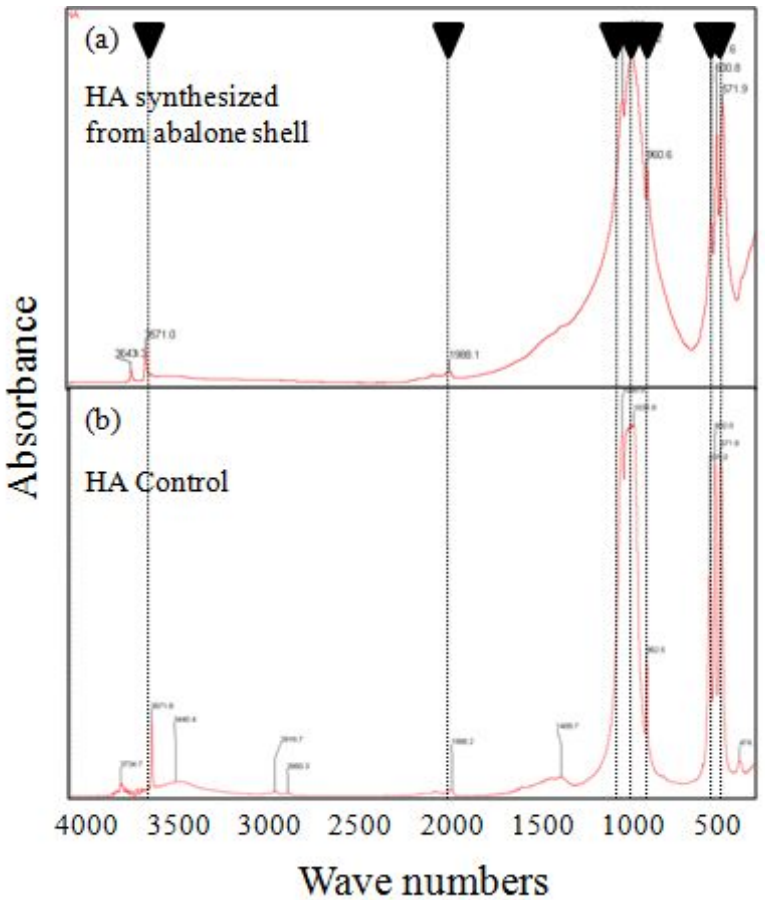

Figure 4. FT-IR analysis of HA obtained at 1230℃. The chemical characteristics were measured by FT-IR (a) HA synthesized from abalone shell, (b) HA Control

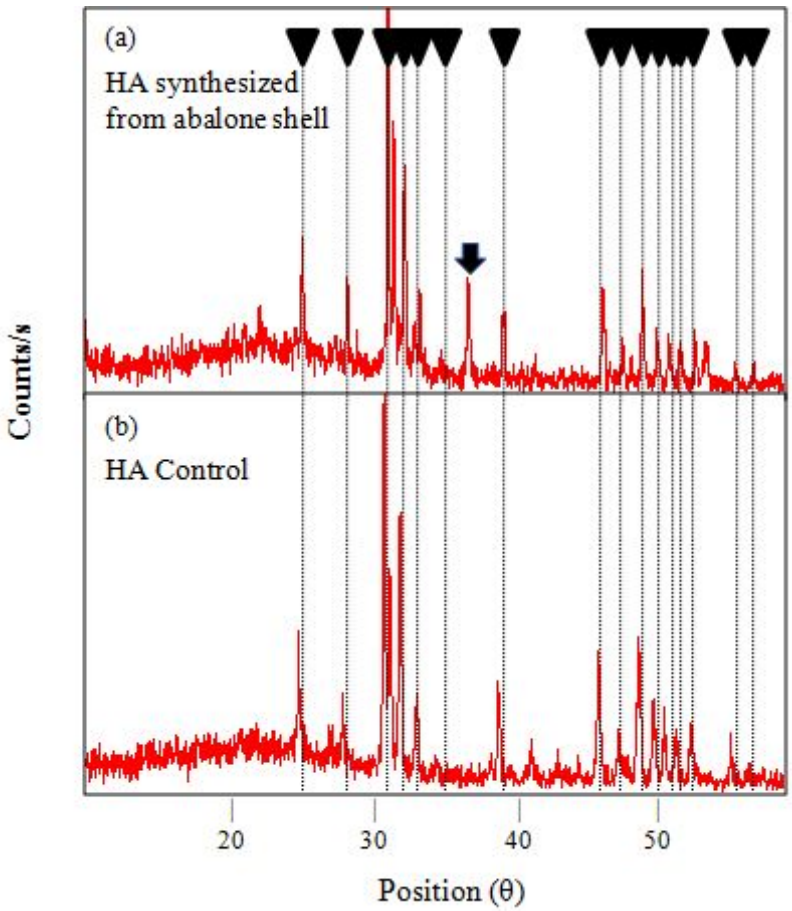

Figure 5. XRD analysis of HA obtained at 1230℃. The crystal structures of the materials were determined by XRD using CuKa radation produced at 40 kV and 30 mA. The patterns were scanned from 10 - 60°, 2Θ at a scan rate of 2° per minute with a step size of 0.05°. (a) HA synthesized from abalone shell, (b) commercial HA (control).

Ⅲ-C. *In vitro* cytocompatibility of abalone shell-derived HA

Ⅲ-C-1. Cytotoxicity of abalone shell-derived HA in MG-63 cells

To determine whether the synthesized HA is cytotoxic, we performed an MTT assay. Human MG-63 osteosarcoma cells were cultured in DMEM medium supplemented with 10% FBS and 1% penicillin/streptomycin in a humidified atmosphere containing 5% CO_2at37°C. The control HA and abalone shell-derived HA were released 3 times in a 10% FBS solution for 72 h each. As shown in Fig. 6, the cells exposed to the abalone shell-derived HA exhibited higher cell viability than the control HA. Therefore, these data suggest that the synthesized HA is relatively nontoxic to MG-63 cells.

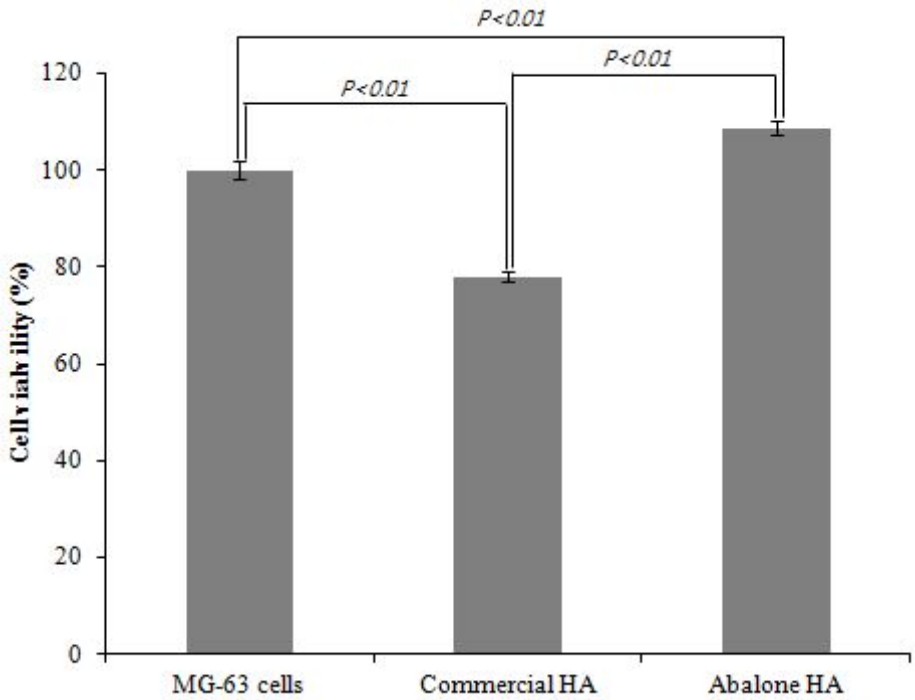

Figure 6. MTT assay of viability of MG-63 osteoblastic cells grown with synthesized HA. Effluents of HA were prepared by the guidelines provided from the Korean Ministry of Food and Drug Safety for the measurement of cytotoxicity. The MG-63 cells were cultured in either DMEM with 10% FBS or the HA effluent, followed by the MTT assay. Data shown are the means ± standard deviation (SD) of three samples ($*p < 0.01$).

Ⅲ-C-2. Cell attachment on the abalone shell-derived HA

Cell attachment to the commercial HA and abalone shell-drived HA was assessed using modified DAPI stain and a cell viability assay. Fig. 7a and b show that cell attachment was verified by DAPI and cell viability assay, respectively. MG-63 cells (5×10^5) were plated with either HA and abalone shell-derived HA on 24-well plates for 24 h. The attached MG-63 cells on the abalone shell-derived HA were visualized by nuclear staining using DAPI under an inverted fluorescence microscope. As shown in Fig. 7a, both commercial and abalone shell-derived HA did not affect the attachment of MG-63 cells.

The cell viability assay was performed to determine the numbers of live and dead cells attached to the commercial HA or abalone shell-derived HA. Live cells, stained green by calcein AM and dead cells stained red by ethidium homodimer-1 were visualized and counted under an inverted fluorescence microscope. As shown in Fig. 7b, MG-63 cells grown in the presence of commercial or abalone shell-derived HA were positively stained via the cleavage of the membrane-permeant calcein AM by the cytosolic esterases in living cells. Furthermore, dead cells stained red by ethidium bromide suggest that abalone shell-derived HA has excellent biocompatibility as a material for bone grafting.

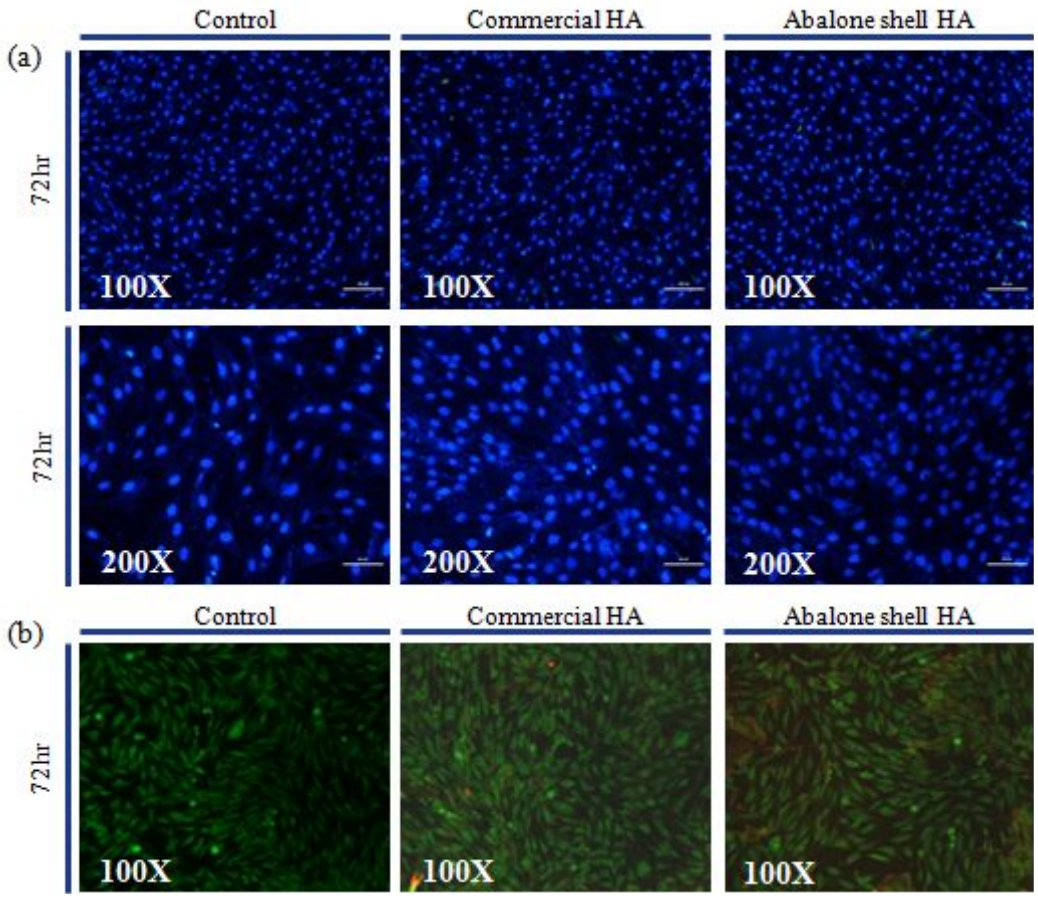

Figure 7. Comparison of cell survival between commercial HA (control) and HA synthesized from abalone shell. Cell survival was evaluated by nuclear staining using DAPI (a), and a LIVE/DEAD cell viability assay (b). Live cells were stained green by calcein AM and dead cells were stained red by ethidium homodimer-1.

Ⅲ-C-3. Osteoinductivity of abalone shell-derived HA in MG-63 cells

To verify the osteoinductivity of abalone shell-derived HA, MG-63 cells were cultured with either commercial or abalone shell-derived HA for 14 days and were evaluated for ALP activity. As shown in Fig. 8, ALP activity in the MG-63 cells cultured with abalone shell-derived HA was higher than in cells grown with commercial HA. At 14 days, ALP activity was verified as 100.49 ± 10.56, 108.67 ± 8.60, and 117.0 ± 8.90 in the MG-63 cells cultured with control, commercial HA, and abalone shell-derived HA effluents, respectively. These results suggest that abalone shell-derived HA exhibits sufficient osteoinductivity for use as a bone grafting bioceramic material.

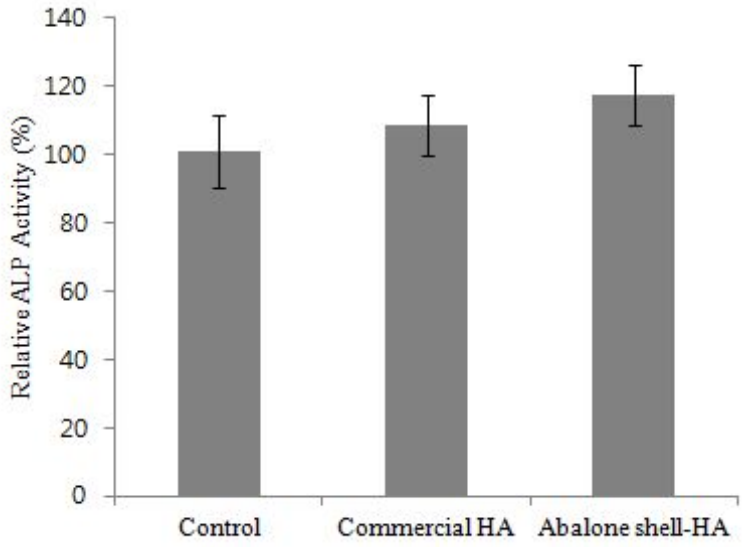

Figure 8. Osteoinductivity of abalone shell-derived HA in MG-63 cells. MG-63 cells were cultured with effluents collected from commercial and abalone shell-derived HA for 14 days. At 14 days, an ALP activity assay was performed to verify the osteoinductivity.

Ⅲ-C-4. Osteoconductivity of abalone shell-derived HA in MG-63 cells

To verify the osteoconductivity of abalone shell-derived HA, MG-63 cells were cultured with abalone shell-derived HA for 4 and 7 days and evaluated for mineralization using alizarin red S staining. As shown in Fig. 9, mineralized nodules were observed in MG-63 cells cultured with both commercial and abalone shell-derived HA for 7 days. Although the level of mineralization in MG-63 cells cultured with abalone shell-derived HA was similar to that of commercial HA, these results suggest that osteoconductivity of abalone shell-derived HA is at least similar to that of the commercial one.

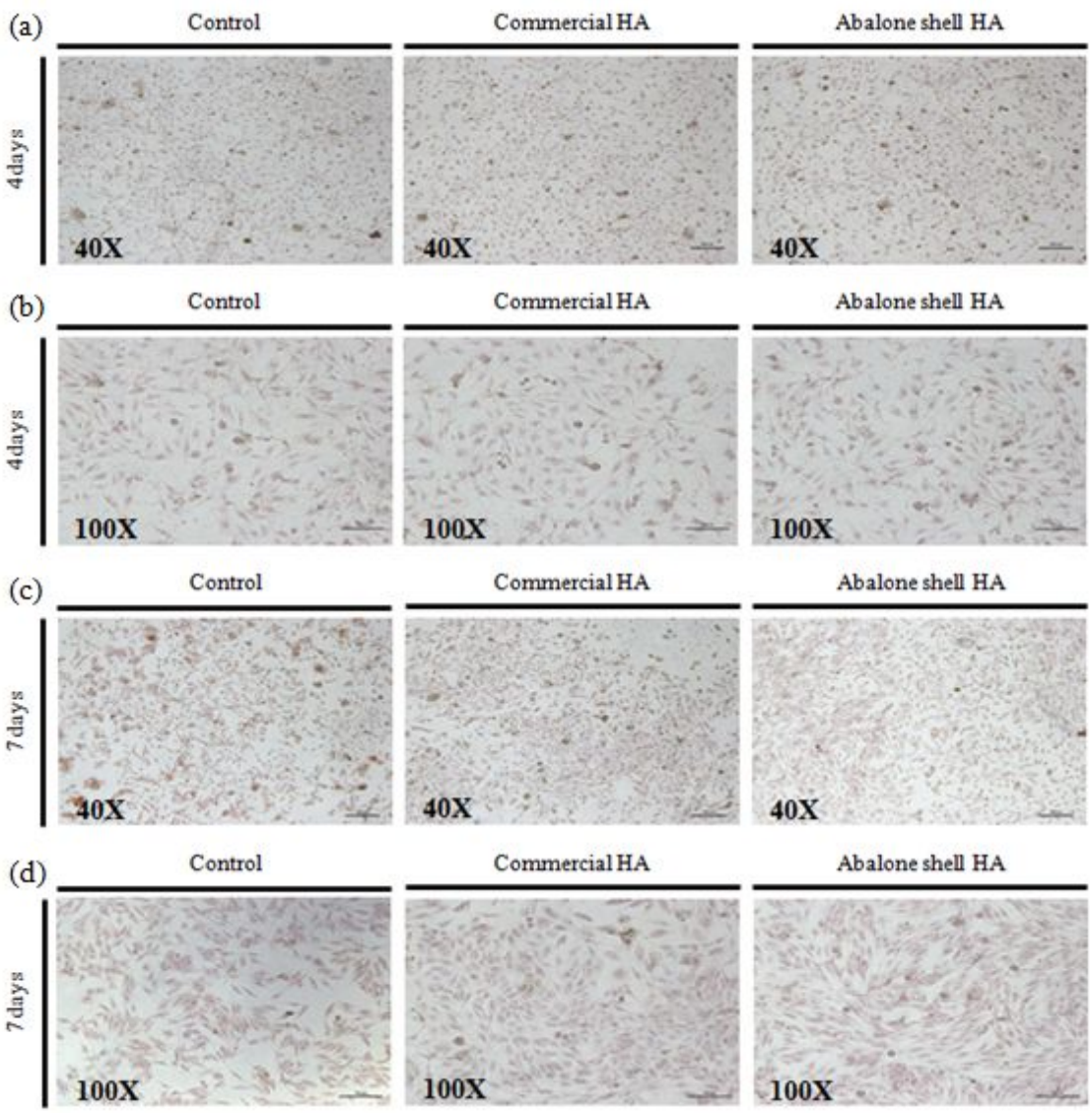

Figure 9. Osteoconductivity of abalone shell-derived HA in MG-63 cells. MG-63 cells were cultured with commercial and abalone shell-derived HA for 4 and 7 days. Osteoconductivity was verified by alizarin red staining and was visualized by optical microscopy at 40× and 100× magnification. (a) 4 days, 40×, (b) 4 days, 100×, (c) 7 days, 40×, (d) 7 days, 100×.

Ⅳ. Discussion

GBR is frequently performed to regenerate bone for implant replacement in dental sugery and usually requires a barrier membrane with bone grafting materials to promote bone healing [9]. The importance of bone grafting materials in GBR has been reported in numerous studies. Bone grafting materials are routinely used to reconstuct bone defects caused by trauma, accident, or infection in oral and orthopedic surgery. Although autologous bone grafting materials have been used as a gold standard, this approach is associated with donor-site morbidity and quantity limitations [10]. To overcome such disadvantages, several biomaterials have been developed as bone substitutes, such as calcium phosphate bioceramics, alumina, zirconia, and bio-glass [11-13].

Calcium phosphate-based biomaterials such as HA and β-tricalcium phosphate have been successfully used for more than 20 years as basic materials for replacing and promoting the reconstruction of damaged or defective hard tissue. HA has chemical and crystallographic similarity to the carbonated apatite of human teeth and bones, and is thus suitable for application in hard tissue replacement. However, despite its excellent biocompatibility and osteoinductivity, the application of HA is limited to non-load-bearing implants and in dentistry because it has poor mechanical properties [14-18].

In this study, the synthesis was dependent on the phosphoric acid and abalone shell-derived calcium oxide sintered at 1230°C for 3 h in an electronic furnace. After sintering, HA formation was observed by SEM. As shown in Fig. 2, the abalone shell-derived HA had a flaky sheet morphology with a sheet size in the range of 25 - 50 μm. These data show that the particle size of abalone shell-derived HA is larger than commercial HA. As shown in Fig. 3, EDS analysis revealed that abalone shell-derived HA contains Na. This is likely due to incomplete washing of the abalone shell-derived HA. However, Fig. 3 shows the

EDS results, which confirm the presence of abalone shell-derived HA with a Ca/P ratio around 1.8, similar to that of the commercial HA. FT-IR and XRD analyses confirmed the composition and crystalline morphology of the HA (Figs. 4 and 5). These results suggest that HA was successfully synthesized successfully from abalone shell at 1230°C.

The MTT assay is commonly used to assess cell viability and the cytotoxicity of bone graft materials. The data in Fig. 6 confirm the lack of detectable cytotoxicity in abalone shell-derived HA effluents, while the commercial HA exhibited some cytotoxicity. Comparison of cell survival in commercial HA and abalone shell-derived HA medium was conducted by DAPI staining and LIVE/DEAD cell viability assay. As shown Fig. 7a, the majority of MG-63 cells were stained blue, indicating intact nuclei. In addition, Fig. 7b shows that the majority of cells were stained green, indicating viability. As shown in Figs. 6 and 7, the MG-63 cells in all samples exhibited high cell viability and survival. These data indicate that both abalone shell-derived HA and commercial HA displayed high levels of biocompatibility.

ALP activity is one of the most important indicators of functional osteoblasts, as differentiated osteoblasts show much higher ALP activity than undifferentiated mesenchymal cells [19, 20]. In this study, the ALP activity of cells cultured with abalone shell-derived HA and commercial HA effluents was assessed for up to 14 days, as shown in Fig. 8. MG-63 cells cultured with ablaone shell-derived HA effluents indicated a significant increase in ALP activity at 14 days as compared to those cultured with commercial HA. Futhermore, as shown by alizarine red S staining in Fig. 9, abalone shell-derived HA induced accelerated mineralization in MG-63 cells. These results demonstrate that abalone shell-derived HA induces cell differentiation.

In this study, we demonstrated the possibility of transforming abalone shell into HA for use as a bone grafting material. We verified that abalone shell-derived HA

can be easily obtained from raw abalone shell by a sintering reaction. The abalone shell-derived HA indicated better biocompatibility than commercial HA. Futhermore, abalone shell-derived HA induced high level of ALP activity in MG-63 cells. These data suggest that abalone shell-derived HA may be a useful bone grafting material for inducing bone healing.

Ⅴ. References

[1] Kang NH, Kim SJ, Song SH, Choi S, Choi SY, Kim YJ. Hydroxyapatite synthesis using EDTA, *J Craniofac Surg.* 2013;24:1042.

[2] Donovan MG, Dickerson NC, Mitchell JC. Calvarial bone harvest and grafting techniques for maxillary and mandibular implant surgery, *Atlas Oral Maxillofac Surg Clin North Am.* 1994;2(2)109-122.

[3] Breine U, Branemark PI. Reconstruction of alveolar jaw bone. An experimental and clinical study of immediate and preformed autologous bone grafts in combination with osseointegrated implants, *Scand J Plast Reconstr Surg.* 1980; 14(1)23-48.

[4] Schmidmaier G, Baehr K, Mohr S, Kretshmar M, Kretschmar M, Beck S, Wildemann. Biodegradable polylactide membranes for bone defect coverage: biocompatibility testing, radiological and histological evaluation in a sheep model, *Clin Oral Implants Res.* 2006;17(4)439-444.

[5] Tayapongsak P, Wimsatt JA, LaBanc JP, Dolwick MF. Morbidity from anterior ilium bone harvest. A comparative study of lateral versus medial surgical approach. *Oral Surg Oral Med Oral Pathol.* 1994;78(3):296-300.

[6] Emmings FG. Chemically modified osseous material for the restoration of bone defects, *J Periodontol.* 1974;45(5):385-390.

[7] Wenz B, Oesch B, Horst M. Analysis of the risk of transmitiing bovine spongiform encephalopathy through bone grafts derived from bovine bone, *Biomaterials.* 2001;22(12):1599-1606.

[8] Lewandrowski KU, Gresser JD, Wise DL, Trantol DJ. Bioresorbable bone graft substitutes of different osteoconductivities: a histologic evaluation of osteointegration of poly(propylene glycol-co-fumaric acid)-based cement implants in rats, *Biomaterials.* 2000;21(8):757-764.

[9] Hammerle CH, Jung RE, Yaman D, Lang NP. Ridgeaugmentation by applying bioresorbable membranes and deproteinized bovine bone mineral : are portof twelve consecutive cases, *Clinical oral implants research.* 2008;19:19-25.

[10] Goulet JA, Senunas LE, DeSilva GL, Greenfield ML. Autogenous iliac crest bone graft. Complications and functional assessment, *Clin Orthop Relat Res*. 1997;(339):76-81.

[11] Heise U, osbron HF, Duwe F. Hydroxyapatite ceramics as a bone substitute, *Int. Orthop.* 1990;14:329-38.

[12] Ackley MA, Monroe E. Alumina as filler for bone cement: a feasibility study, *Biomaterials*. 1980;1(4):217-21.

[13] Stanic V, Aldini NN, Fini M, Giavaresi G et al. Osteointegration of bioactive glass-coated zirconia in healthy bone: an in vivo evalutaion, *Biomaterials*. 2002;23(18):3833-41.

[14] Goller G, Oktar FN, Agathopoulos S, Tulyaganov DU, Ferreira JMF, Kayali ES, Peker I. The influence of sintering Temperature on Mechanical and Microstructural Properties of Bovine Hydroxyapatite, *Key Engineering materials*. 2005;284-286:325-328.

[15] Erkmen ZE, Genc Y, Oktar FN. Microsturctural and Mechanical Properties of Hydroxyapatite-Zirconia Composites. J Am. Ceram. Soc. 2007;90:2885-2892.

[16] Oktar FN, Yetmez M, Agathopoulos S, Lopez Goeme TM, Goller G, Peker I, Ferreira JMF. Bond-coating in plasma-sprayed calcium-phosphate coating, *J. Mater. Sci. Mater. Med.* 2006;17(11):1161-1171.

[17] Oktar FN, Goller. G, Yetmez M, Toykan D. Effects of Bond-coatings on plasma sprayed calcium phosphate coatings, *Key Engineering Materials*. 2003;240-242:315-315.

[18] Oktar FN, Agathopoulos S, Ozyegin LS, Gunduz O, Demirkol N, Bozkurt Y, Salman S. Mechanical properties of bovine hydroxyapatite (BHA) composites doped with SiO2, MgO, Al2O3, and ZrO2, *J. Mater. Sci. Mater. Med.* 2007;18(11):2137-2143.

[18] Oktar FN, Agathopoulos S, Ozyegin LS, Gunduz O, Demirkol N, Bozkurt Y, Salman S. Mechanical properties of bovine hydroxyapatite (BHA) composites doped with SiO2, MgO, Al2O3, and ZrO2, *J. Mater. Sci. Mater. Med.* 2007;18(11):2137-2143.

[19] Verron E, Bouler JM, Guicheux J. Controlling the biological function of calcium

phosphate bone substitutes with drugs, *Acta biomaterialia*. 2012;8(10):3541-3551.

[20] Liu M, Yao S, Yang L, Mengtong Y, Zhihui Z, Weiping H. Modulation of the differentiation of Dental Pulp stem cells by different concentrations of beta-glycerophosphate, *Molecules*. 2012;17:1219-1232.

감사의 글

먼저 제가 가장 존경하고 사랑하는 우리 아버지 강 성철 사장님과 어머니 김 명옥 여사님. 항상 아들을 이끌어주시고 믿음으로 지켜봐 주셔서 감사합니다. 두 분 덕분에 제가 많은 복을 받고 있는 것 같습니다. 앞으로도 베풀어 주신 은혜에 감사드리며 사는 아들이 되도록 하겠습니다. 석사 학위 기간 동안 학문의 길을 이끌어주시고 제자로써 아껴주셨던 존경하는 김수관 지도 교수님께 깊은 감사를 드립니다. 학부생 때부터 사랑과 애정으로 지도해 주시고 많은 관심으로 보살펴 주시는 이숙영 교수님 감사드립니다. 그리고 힘들어 할 때나, 고민이 있을 때 늘 곁에서 아낌없는 조언과 격려를 통해 도움을 주시고, 다양한 기회를 주신 김재성 교수님께 항상 감사드립니다.

그리고 저를 친동생처럼 아껴주고, 다양한 경험으로 저를 성장시켜준 우리 정강이 형님과, 승찬이 형님, 제가 항상 괴롭히지만 실험실의 상생의 덕을 보여주고 있는 임선생, 나이 많은 후배 챙기느라, 실험 가르쳐주느라 고생 많이 한 맞선배 오실장님, 맞 후배로 항상 긍정적인 실험실의 모범이 되어주는 조인아 선생님, 육아와 업무에 힘든 와중에도 매일 웃는 모습이 변함없이 예쁜 복희, 수식어가 필요 없는 실험실의 내 동생 현정이 모두 감사드립니다.

그리고 늘 따뜻하게 대해주시고, 저의 학위 논문 작성에 많은 지도를 해주셨던 김도경 교수님, 모든 면에서 만능으로 멋지신, 김춘성 교수님, 틈날 때마다 실험적, 진로적 문제에서 많은 조언 해주셨던 문성민 박사님. 세 분의 가르침과 지도 덕분에 많은 것을 배울 수 있었습니다. 감사합니다.

모든 분들께 언제나 감사하고, 앞으로의 일에도 두려움 없이 도전 하는 사람으로 한걸음씩 천천히 나아가도록 하겠습니다. 감사합니다.